7th International DAAAM Baltic Conference
"INDUSTRIAL ENGINEERING
22-24 April 2010, Tallinn, Estonia

FEM MODELLING OF MICROHOLES LASER BEAM AND ELECTRODISCHARGE MACHINING AIDED BY ULTRASONICS

Marinescu, N.I; Ghiculescu, D. & Nanu, S.

Abstract: *The paper deals with Finite Element Method (FEM) comparative modelling of microholes machining with diameters of 0.1 mm order through four types of technologies: classic percussion laser beam machining (LBM) and aided by ultrasonics (+US), classic electrodischarge machining (EDM) and aided by ultrasonics (+US). The FEM modelling of combined roughing LBM and finishing EDM in two cases – classic and ultrasonic aiding - is also approached proving that this combination is able to get both advantages of LBM and EDM.*
Key words: microholes, LBM, EDM, ultrasonics.

1. INTRODUCTION

Comparative Finite Element Modelling (FEM) of microholes machining with diameters of 0.1 mm order was approached using four types of machining: percussion laser beam machining (LBM), electrodischarge machining (EDM) and both aided by ultrasonics (LBM+US, EDM+US). The FEM modelling is based on phenomenology of these four types of removal mechanisms. Micro/finishing EDM+US phenomenology is detailed in our previous papers [1], [2], and the classic technologies are the subject of many papers provided by the state of the art, e.g. Van Dijck et al. [3], [4], for EDM and many others for LBM, synthesized in [5], [6].
The goal of our researches is the optimization of microholes machining within materials with usual low machinability in terms of machining rate, precision and surface quality.
MicroLBM modelling consists in roughing by five consecutive 200 ms, 80 J high energy pulses of Nd:YAG laser, generating a microhole of 0.2 mm radius and around 1 mm depth within a tool steel, X210Cr12. MicroEDM is also used for hole surface finishing with 0.8 A current, 25 μs pulse time and wire/microtubular electrode-tool. The aiding by ultrasonics supposes 20 KHz frequency vibrations of workpiece at LBM and of tool at EDM.

2. PHENOMENOLOGY AND MACHINING PARAMETERS

A more detailed analysis of specific phenomena concerning LBM+US is presented, taking into account that this technology is less usual.
The thermal phenomena are dominant within machining mechanism. The role of US aiding is to intensify the material thermal removal through cavitational phenomena. Taking into account Gaussian distribution of laser intensity and absorption phenomenon within the machined material, then, in a point with coordinates (r, z) (fig.1), the intensity of laser radiation I (r, z) can be determined with the relation [7]:

$$I(r,z) = I(0,0) \cdot e^{-\frac{2r^2}{r_0^2+(\theta \cdot z)^2}} e^{-\alpha \cdot z} \text{ [W/cm}^2\text{]} \quad (1)$$

where: $I(0, 0)$ is the intensity from the origin (0, 0); α - absorption coefficient of material to be machined; r_0 - spot radius focused on the material to be machined; θ - angle of focalization cone.

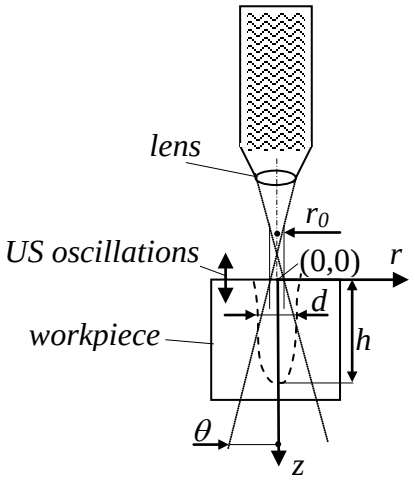

Fig.1. LBM parameters used for modelling of microholes machining

Even if the intensity I is not uniform on laser spot, it is able to produce a very high temperature on thermally attacked surface, especially in case of relative long pulses as in the present case. However, the spot temperature cannot be greater than material boiling point. Therefore, at FEM boundary conditions, the spot temperature is considered uniform and equal with maximum temperature, i.e. boiling point.

At each pulse, the laser spot is focused above the machined surface, keeping the spot (r_0) at a necessary value to generate the prescribed diameter of microhole and the workpiece is vibrated with very small amplitude (A) of μm order, sufficient to exceed the cavity threshold [2]. This depends on the nature of the liquid in which cavitation is induced, viscosity, number of cavitation nuclei etc.

Theoretically, the microhole depth (h) can be determined with the relation [8]:

$$h \cong \frac{Wt_i}{\pi r_0^2 L_0} \quad [\text{mm}] \qquad (2)$$

where: W is laser beam power; t_i – pulse time; L_0 – removal specific energy (heating, melting, vaporization of volume unit). Similarly, the microhole radius (r) resulted from relation [8]:

$$r = r_0 + \frac{Wt_i \cdot tg\gamma}{\pi r_0^2 L_0} \quad [\text{mm}] \qquad (3)$$

where γ is the angle between laser beam direction and the tangent at hole surface.

The minimum laser spot d_0 depends on optical system characteristics and practically, it varies according to the relation:

$$d_{0min} = 2...5\ \lambda \quad [\mu\text{m}] \qquad (4)$$

where λ is the wave length.

In case of Nd:YAG laser used in our researches, the following parameters were used: W=400W; pulse energy, E=80J, λ =1.06 μm, t_i=200 ms, r_0= 30 μm.

The cavitational phenomena ultrasonically induced within the melted material from the microhole during the pulse time t_i have great influence on removal mechanism. The acoustic pressure (p_{ac}) oscillates during two ultrasonic semiperiods, as the following relation shows:

$$p_{ac} = 2\pi \cdot z \cdot f_{US} \cdot c \cdot \rho \quad [\text{mm}] \qquad (5)$$

where z is the elongation on vertical direction, normal on machined surface; $z=A\sin\omega t$; f_{US} – ultrasonic frequency; c – sound velocity within the liquid material; ρ – density of melted material.

The ultrasonic oscillations act like an additional pump mechanism, increasing the evacuation of melted material from microcavity. In the liquid stretching semiperiod when the acoustic pressure lowers, becoming negative due to negative elongation (z), vaporization temperature (T_{vap}) and melting temperature (T_{melt}) decrease, increasing the removed volume that is easier evacuated by increased pressure at the beginning of the liquid compression semiperiod. The US effect on T_{melt} is more reduced in comparison with the one produced on T_{vap}. For steel, temperature difference can be ΔT_{vap} = 45°C if the pressure is p_{vap}=0.1 Mpa, T_{vap} = 2880°C and increasing of pressure due to p_{ac} is Δp_{ac} =2x 10^4 Pa [9]. The effects of these phenomena can be observed in difference of microhole dimensions obtained with and without US assistance.

Machining	LBM		LBM+US	
Directions	Depth [mm]	Radius [mm]	Depth [mm]	Radius [mm]
Microhole	9.5	0.2	1.1	0.2
Melting isothermal	1.117	0.24	1.157	0.24
Max. Ratio removed/melted	0.85	0.83	0.95	0.83

Table 1. Experimental data – microhole dimensions obtained by Nd:YAG 5 pulses

The comparative data of five pulses LBM and LBM+US are presented in table 1.

A very obvious inferiority of μEDM machining rate compared to LBM, more than 1300 times in this case, is mainly explained in terms of pulse energy. Working with 0.8 A current and 25 μs pulse time, the pulse energy is around 0.4 mJ. This low energy is imposed by reduced frontal area of tubular or wire electrode that is used in this case related to current density [10].

Moreover, the removal mechanism is based mainly on boiling at the end of the pulse, according to Van Dick's model [3], confirmed by FEM modelling and our experimental data.

The melted material is overheated, 200-300°C, above the boiling point, but the material is removed through boiling only after the end of the pulse when the pressure suddenly lowers. This leads to low efficiency of classic EDM, under 10%.

When EDMing with ultrasonics aiding, an increasing with up to 500% of machining rate could be possible if some optimization conditions of working parameters are met [1]. If the collective implosion of the gas bubbles from interlectrode gap (cumulative microjets stage) occurs in few μs after the pulse end (depending on t_i), the hydraulic forces find an important part of material in liquid state and can remove it. Otherwise the melted material is resolidified.

Machining	EDM		EDM+US	
Directions	Depth [μm]	Radius [μm]	Depth [μm]	Radius [μm]
Crater	3.8	5	3.2	4

Table 2. Experimental data – EDM microcraters mean dimensions, I=0.8 A, t_i=25μs, negative polarity.

However, the material can be removed in solid or plastic state by high ultrasonic pressure, of 10 MPa order, contributing thus to significantly ameliorate low μEDM machining rate and improving the surface quality.

The reference experimental data obtained when working with commanded pulses with lowest step of current (I) - due to very low section of electrode-tool - of Romanian ELER01 machine are synthesized in table 2.

3. FEM MODELLING

The FEM Modelling was achieved using Comsol Multiphysics, Transient Heat Transfer Module for thermal removal analysis, coupled with Structural Mechanics, Plane Stress Transient Analysis for ultrasonics removal study.

In the first stage, 2D geometry was created as shown in fig. 2, in order to save computational resource taking into account the symmetry of modelled phenomena. The workpiece was a square of 10 mm. PT1 and PT2, on its superior surface, defined the size of laser spot of 2x0.030 mm. PT3 and PT4 described the position of assist gas jet with diameter 2x1mm.

Each pulse removed an ellipsoidal cavity whose dimensions were determined by position of melting isothermal and the ratios removed/melted volumes (Table 1).

Segments B1, B2, containing PT1 and PT2, were drawn to allow the laser spot focusing on the current crater bottom at each pulse.

Meshing based on Lagrange-T_2J_1 triangular elements was refined in the zone adjacent to laser spot.

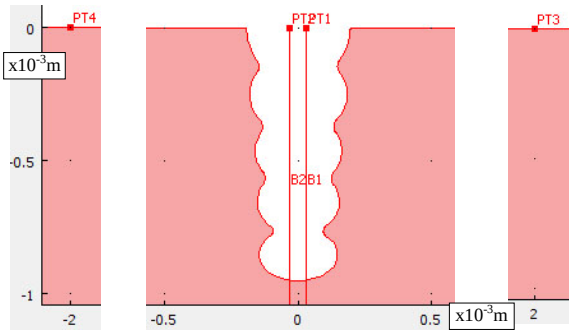

Fig. 2. Geometry parameters at LBM (+US)

Thermal properties of X210Cr12 (D3 DIN) from Comsol Multiphysics library are temperature dependent.

As boundary settings, spot laser temperature of 3273 K, equal with steel boiling point was imposed on PT1-PT2. The high power of laser radiation is able to raise to maximum value the spot temperature on the very most part of this surface despite its Gaussian distribution. Thermal insulation, corresponding to assist gas spot, was set on PT3-PT4, including microhole border. The rest of boundaries, belonging to workpiece were set at ambient temperature. Previous program runnings emphasized that overall workpiece dimensions of mm order have not influenced the temperature distribution.

The roughing LBM cycle of modelling comprised five 200 ms pulses (t_i), each of them followed by 50 ms cooling for the period of pause time (t_o).

During the LBM percussion cycle the machined material accumulates thermal energy. For example, after the first pulse 50 ms cooling, the temperature inside the material is still high, i.e. over 783K. So, the second pulse benefits from the temperature created by the first pulse.

Temperature distribution after the five successive heating-cooling pulses cycle at LBM is presented in fig. 4. The maximum temperature after cooling was over 947K. Although this maximum temperature rose progressively at pulses number increase, the removal rate lowers gradually.

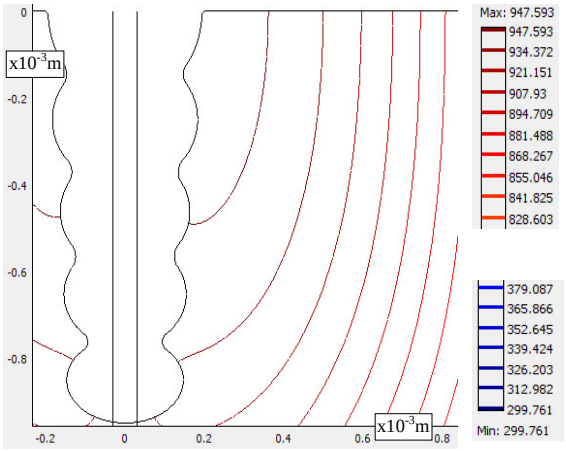

Fig. 4. Temperature [K] distribution after the fifth 50 ms cooling at LBM

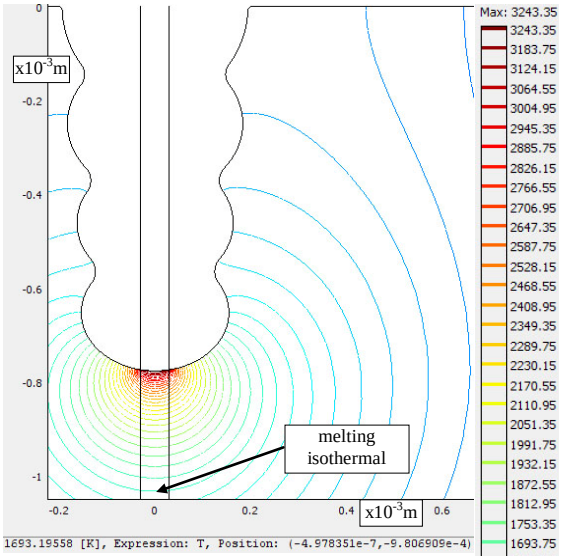

Fig. 5. Temperature [K] distribution after the fifth 200 ms pulse at LBM

The decrease of crater volume at the hole bottom is due to increase of adjacent volume to laser spot on which pulse energy is distributed.

An important diametric aberration of around 0.1 mm resulted from melting isothermals (1693K) disposal (fig. 5) and ratio removed/melted volume from table 1. This aberrance will be corrected by EDM.

LBM+US five pulses cycle emphasised some improvement of machining rate in agreement with experimental data from table 1, i.e. removal/melted ratio. The diametric aberrance also decreased to 0.06 mm approximately, so the task of EDM to correct it becomes easier (fig.6).

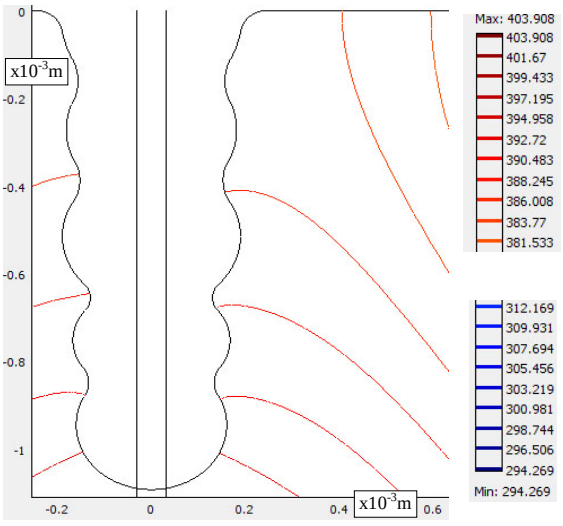

Fig. 6. Temperature [K] distribution after the fifth 50 ms cooling at LBM+US

Comparing to final temperature distribution at five pulses classic LBM, (fig.4), the ultrasonic assistance produced decrease of this temperature, i.e. thermal energy was consumed to evacuate a greater amount of material. As in previous machining type although the temperature after each cycle of cooling increased from around 397K to over 403K, the volume removed by each pulse decreased gradually at the microhole bottom, due to growing of surrounding absorbing thermal energy.

The geometry for EDM (+US) modelling comprised a vertical segment, containing PT3 to define lateral gap (s_L) at 10 μm from final diameter (0.2 mm), horizontal segments (B_i) describing successive positions of EDM spots on LBMed surface (fig. 7). Point PT4 and homologous one PT5 (not shown) on workpiece surface represent the limits of gas bubble of 0.1 mm order around the plasma channel [2].

As boundary conditions, the EDM spots were loaded with 3573K, 300 degrees above boiling temperature, i.e. 3000°C [3]. The PT4-PT5 curve around the spot was considered as thermal insulation. The exterior surfaces of 10 mm workpiece surface were set to 313K, the temperature of dielectric liquid during machining.

At classic μEDM, first discharges produced low craters depth. After previous discharges (craters overlap), crater depth increases (becoming closer to experimental data - table 2), the volume on which thermal energy is distributed being lower.

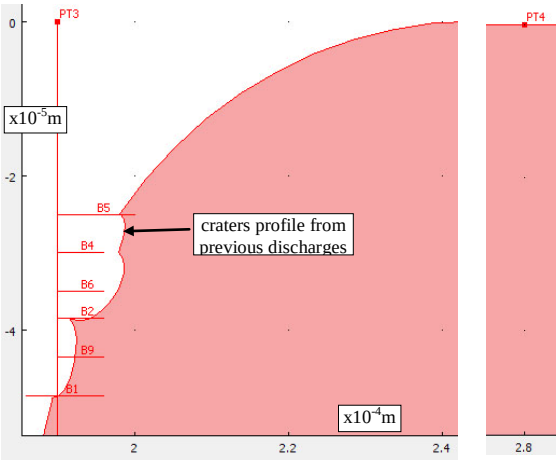

Fig.7. Geometry parameters at EDM (+US)

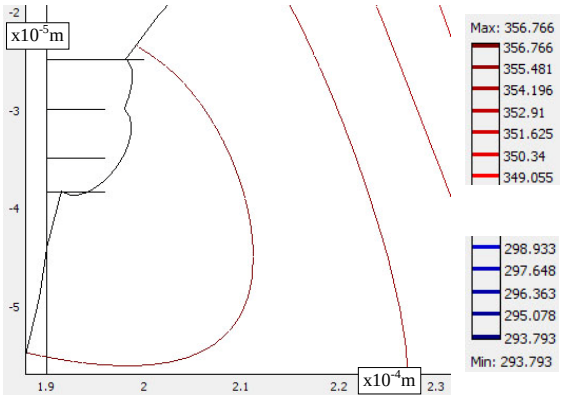

Fig. 8. Temperature [K] distribution after 100μs from 25μs pulse end - classic EDM

Due to long delay time (100 μs) between finishing discharges, all melted material after discharge is already solidified - 356K, highest temperature (fig. 8) - when dielectric liquid access the EDM spot, so EDM efficiency is very low.

At EDM+US, if collective implosion of gas bubbles from the gap occurs around 1 μs, after pulse end, the hydraulic forces of dielectric liquid still find material in liquid state - 1693K melting isothermal (fig. 9) - and remove this volume. Thus an important increasing of machining rate can be achieved by synchronization between commanded pulses and US oscillations. Otherwise the shock waves produced by bubbles collective implosion of 10 MPa order can remove up to 50% from height of solid crater margin (D3 steel ultimate tensile strength, 1500 MPa) when the walls between craters are thin enough (craters overlap) (fig. 10). These FEM results were obtained by coupling transient thermal and mechanical modules of Comsol.

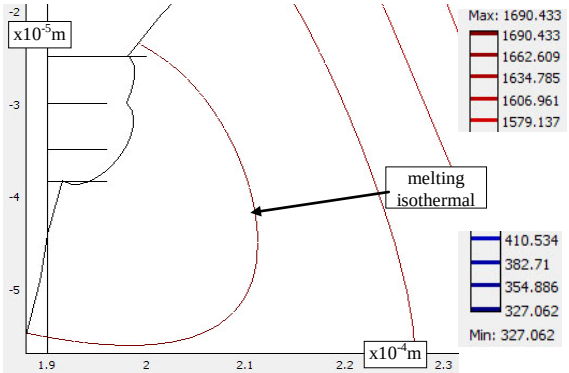

Fig. 9. Temperature [K] distribution after 1.2 μs from 25 μs pulse end - EDM+US

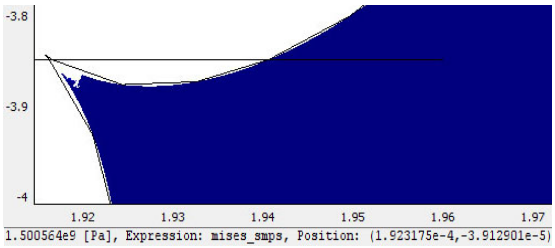

Fig.10. Von Mises stresses [Pa] at 90 MPa shock waves pressure on craters margin

As boundary conditions, the margins of EDM crater were loaded to 50 MPa since shock waves are directed along microhole axis and fixed constraints were imposed on inferior and lateral sides of workpiece due to fixing system during machining. The results leading to decrease of surface roughness up to 50% are in agreement with experimental data [10].

4. CONCLUSION

The FEM modelling results indicated that appropriate combination in terms of machining rate, precision and surface quality of microholes could be roughing LBM+US and finishing EDM+US. LBM+US improves machining rate with around 10% and reduce diametric aberrance up to 50% comparing to classic LBM. EDM+US is able to raise machining rate more than five times if synchronization between commanded pulses and tool US oscillations is achieved. EDM+US is also able to correct the imprecision of previous LBM and to improve surface roughness up to 50% comparing to classic EDM. These could be attained only under some optimization conditions of working parameters.
EDM+US dedicated equipment for microholes previously LBMed is the subject of our further researches.

5. REFERENCES

1. Ghiculescu, D. Marinescu, N. I., Jitianu, G., Seritan, G., On precision Improvement by Ultrasonics-aided Electrodischarge Machining, *Estonian J. of Eng.*, 2009, **15, 1,** 24-33.

2. Marinescu, N. I., Ghiculescu, D. Jitianu, G., Solutions for Technological Performances Increasing at Ultrasonic Aided Electrodischarge Machining, *Int. J. Mater. Form.*, 2009, **2**, 681–684.

3. Van Dijck, F., Snoeys, R., Theoretical and Experimental Study of the Main Parameters Governing the Electrodischarge Machining Process, *Mecanique*, 1975, **301-302**, p. 9-16.

4. Van Dijck, F., Snoeys, R., Metal Removal and Surface Layers in Electrodischarge Machining, *Int. Conf. On Prod. Eng. Proc*, 1974, Tokyo, Japan Soc. Prec. Eng, 46-50.

5. Meijer, J. Laser beam machining (LBM), state of the art and new opportunities, *J. Mater. Process. Tech.*, 2004, **149**, 2–17.

6. Dubey, A. K, Yadava, V. Laser beam Machining - A review, *International Journal of Machine Tools & Manufacture*, 2008, **48**, 609-628.

7. Marinescu, N. I. et al. *Treatise of Nonconventional Technologies, Ultrasonics Machining*, Bren, Bucharest, 2004.

8. Marinescu, N. I. et al. *Machining Processes with Beams and Jets*, INOE Bucharest, 2000.

9. Yue et al. Analysis of Ultrasonic-Aided Laser Drilling Using Finite Element Method, *Annals of the CIRP*, 1996, **45,** 169-172.

10. Ghiculescu, D. *Nonconventional Machining*, Printech, Bucharest, 2004.

6. ADDITIONAL DATA ABOUT AUTHORS

Marinescu, Niculae, Prof., Ph.D; e-mail: niculae.marinescu@yahoo.com
Ghiculescu, Daniel, Assoc. Prof., Ph.D.;
e-mail: liviudanielghiculescu@yahoo.com
Nanu, Sergiu, Eng.,
e-mail: sergiu.nanu@nsn.pub.ro
University "Politehnica" of Bucharest; Splaiul Independentei 313, sector 6, Bucharest, Romania, http://www.pub.ro; phone: 0040 402 9373.